Applied Thermal Engineering 289 (2026) 129899

Contents lists available at ScienceDirect

Applied Thermal Engineering

journal homepage: www.elsevier.com/locate/apthermeng

Research Paper

Pyrolysis mechanism and radical evolution in $C_6F_{12}O$–N_2 gas mixtures: A combined ReaxFF MD and DFT study

Kai Wang [a,b], Dezheng Wang [a,b], Bin Zheng [c], Wei Wang [d], Biao Zhou [a,b,*]

[a] Inner Mongolia Research Institute, China University of Mining and Technology (Beijing), Ordos 017010, PR China
[b] School of Emergency Management and Safety Engineering, China University of Mining and Technology (Beijing), Beijing 100083, PR China
[c] Department of Fire Protection Engineering, China Fire and Rescue Institute, Beijing 102202, PR China
[d] Laboratory of Fire-fighting Theory, Shanghai Fire Science and Technology Research Institute of MEM, Shanghai 200032, PR China

ARTICLE INFO

Keywords:
Pyrolysis mechanism
$C_6F_{12}O$
Free radical chain reaction
Density functional theory
ReaxFF–MD simulation

ABSTRACT

Perfluorohexanone ($C_6F_{12}O$) is a clean fire suppressant and is often used together with nitrogen (N_2), but the thermal pyrolysis behavior and radical evolution in $C_6F_{12}O$–N_2 mixtures are still not well understood. Previous studies mainly considered discharge conditions or other buffer gases and rarely combined experiments with multi-scale simulations. This study integrates tubular-furnace experiments, density functional theory (DFT) and ReaxFF molecular dynamics (MD) to clarify the dominant pyrolysis pathways of $C_6F_{12}O$–N_2 and the effects of operating conditions. Experiments at 450–750 °C show that significant $C_6F_{12}O$ pyrolysis starts near 550 °C, with products evolving from higher perfluoroalkanes (C_5F_{12}, C_4F_{10}, C_3F_8) to smaller fluorocarbons (C_3F_6, CF_4) as temperature increases. DFT indicates that C—C bonds adjacent to the carbonyl group are the weakest, leading to primary radicals C_3F_7·, C_2F_5· and CF_3·, which explain the observed product spectrum. ReaxFF-MD reproduces these trends and resolves the time-dependent evolution of radicals under different temperature, mixing-ratio and pressure conditions. A moderate N_2 fraction promotes initial activation of $C_6F_{12}O$, whereas excessive N_2 or high pressure suppresses radical chain propagation and lowers the pyrolysis extent. The identified endothermic bond scission and fluorinated radicals that scavenge H·/OH· radicals provide mechanistic support for the combined cooling and chemical-inhibition effects responsible for fire suppression by $C_6F_{12}O$–N_2 mixtures.

1. Introduction

Traditional halon fire extinguishing agents have been listed for phase-out by the Montreal Protocol due to their ozone-depleting effects, searching for halon alternatives is an important research direction in the fire protection field [1,2]. With increasingly stringent environmental regulations, new agents are required to combine high fire-suppression efficiency with low toxicity, electrical non-conductivity and minimal environmental impact, particularly in high-value or safety-critical applications such as data centres, aircraft cargo compartments and cultural heritage protection. Perfluoro-2-methyl-3-pentanone ($C_6F_{12}O$) is one of the new generation halon replacement extinguishing agents that has garnered increasing attention for its favorable physicochemical and environmental properties. It is a colorless, odorless, transparent liquid at room temperature with an ozone depletion potential (ODP) of 0, a global warming potential (GWP) of 1, and an atmospheric lifetime (ALT) of 0.014 years [3]. These values reflect its low environmental impact and short atmospheric persistence, allowing it to degrade relatively quickly compared to traditional halocarbons [4,5]. In addition, $C_6F_{12}O$ exhibits high extinguishing efficiency, low acute toxicity, negligible residue after discharge and convenient storage and transport, and it has already been deployed in various total-flooding and local fire suppression systems. However, previous studies have shown that $C_6F_{12}O$ can promote flame propagation under certain conditions; at relatively low concentrations, it may enhance combustion in special scenarios such as aircraft cargo holds, potentially causing an overpressure risk [6,7]. Furthermore, pyrolysis of $C_6F_{12}O$ during fire suppression may generate hazardous byproducts, notably hydrogen fluoride (HF) and carbonyl fluoride (COF_2), both of which are toxic and corrosive [8]. Long-term degradation of $C_6F_{12}O$ in the environment can also produce persistent fluorinated byproducts such as trifluoroacetic acid (TFA) and trifluoromethane (HFC-23). These substances are known for their potential to cause secondary environmental pollution and bioaccumulation concerns [9]. Therefore, a deeper understanding of its

* Corresponding author at: Inner Mongolia Research Institute, China University of Mining and Technology (Beijing), Ordos 017010, PR China
E-mail address: zhoubiao1088@cumtb.edu.cn (B. Zhou).

https://doi.org/10.1016/j.applthermaleng.2026.129899
Received 4 October 2025; Received in revised form 6 December 2025; Accepted 21 January 2026
Available online 24 January 2026

pyrolysis mechanism under fire conditions is therefore essential for the safe and rational use of $C_6F_{12}O$-based systems.

To address the limitations of using $C_6F_{12}O$ alone, recent work has explored synergistic combinations with other gases or extinguishing technologies [10,11]. The goal is to enhance fire suppression performance, reduce the required agent concentration, and mitigate harmful pyrolysis products [12,13]. Rapid atomization of $C_6F_{12}O$ has been shown to increase its heat-absorption and cooling capability, giving a cooling performance slightly lower than 2-BTP but higher than HFC-227ea and Halon 1301 [14]. Gas-mixture strategies have also been investigated: simulations of $C_4F_7N/CO_2/O_2$ systems using DFT and reactive MD demonstrated that adding O_2 advances the onset of C_4F_7N pyrolysis while reducing major decomposition products, suggesting routes to composition optimisation [15]. Nitrogen has been evaluated as an environmentally benign agent for aircraft cargo fires, where its combination with water mist can satisfy FAA performance requirements while maintaining good suppression efficiency and eco-compatibility [16]. In parallel, thermally triggered microcapsules encapsulating $C_6F_{12}O$ in flame-retardant resin have been developed to realise rapid release and efficient suppression in confined spaces. [17]. On the mechanistic side, several works have examined the decomposition of perfluoroketones and related gases in mixed systems. The by-products of $C_6F_{12}O$–N_2 and $C_6F_{12}O$–air under AC corona discharge have been characterised by GC–MS with a focus on insulation performance and toxicity, but without resolving the underlying thermal pyrolysis network or radical chain processes [18,19]. Other studies used ReaxFF-MD to analyse the discharge-driven pyrolysis of $C_5F_{10}O$–air and $C_6F_{12}O$–CO_2 mixtures, revealing strong temperature dependence and identifying major products and pathways under gas-insulated equipment conditions [20]. Overall, these investigations confirm that $C_6F_{12}O$ can work effectively when combined with N_2 or other gases, yet the purely thermal pyrolysis mechanism of $C_6F_{12}O$-N_2 mixtures under fire-like conditions has not been systematically clarified. Quantitative information on the onset temperature, dominant bond-breaking routes and radical evolution is still limited, and multi-scale, experimentally supported descriptions of the reaction network are lacking. Moreover, the coupled influences of temperature, $C_6F_{12}O$-N_2 mixing ratio and pressure on pyrolysis extent and radical populations have not been summarised in a unified way, which hampers rational optimisation of key design parameters for $C_6F_{12}O$-N_2 fire-extinguishing systems. Therefore, a systematic study of the pyrolysis mechanism and influencing factors of $C_6F_{12}O$-N_2 gas mixtures is of significant importance.

To promote the safety and environmental friendliness of $C_6F_{12}O$ use, this study systematically investigates the pyrolysis mechanism and influencing factors of the $C_6F_{12}O$-N_2 gas mixture, using a combined approach of high-temperature pyrolysis experiments, density functional theory (DFT) calculations, and reactive force field molecular dynamics (ReaxFF-MD) simulations to reveal how N_2 alters the thermal degradation of $C_6F_{12}O$, the pyrolysis mechanism and influencing factors of $C_6F_{12}O$-N_2 mixed gas were systematically studied. Key pyrolysis intermediates and free radical species were identified, and the main bond-breaking pathways of the mixed gas and the role of key free radicals in the chain reaction were elucidated. The main influences of temperature, $C_6F_{12}O$-N_2 mixing ratio, and pressure on the degree of pyrolysis, product distribution, and free radical evolution were revealed. The results provide new mechanistic insights into the pyrolysis of $C_6F_{12}O$-N_2 and serve as reference data for optimizing the composition and operating conditions of mixed gas fire extinguishing agents.

2. Methodology

2.1. High-temperature pyrolysis experimental platform

To study the pyrolysis characteristics of the $C_6F_{12}O$-N_2 gas mixture, an appropriate high-temperature pyrolysis experimental platform is constructed, as illustrated in Fig. 1. The platform mainly consists of a reactant intake system, high-temperature resistant reaction tube, temperature-controlled heating device, gas drying and acid removal unit and sample collection and analysis system. The main instruments include gas mass flow controller, syringe pump, tubular muffle furnace, K-type thermocouple, automated sampling system and gas chromatography–mass spectrometry (GC–MS). In the experiment, mixtures of $C_6F_{12}O$ and N_2 at different ratios are mixed through the pyrolysis tube and heated to the set furnace temperature (450–750 °C) to simulate the actual fire temperature, with an effective residence time of 4 s in the constant temperature hot zone. The collected product samples are analyzed by GC–MS. The GC–MS testing conditions are as follows, the chromatographic column is KB-PFXN (150.0 m × 0.32 mm × 2 μm); the initial temperature is 35 °C held for 5 min, followed by heating at 10 °C/min to 150 °C and holding for 10 min; helium is used as the carrier gas at a flow rate of 1.2 mL/min with a split ratio of 80:1; the mass spectrometer uses an electron impact ion source with an energy of 70 eV, an ion source temperature of 250 °C, a quadrupole temperature of 150 °C, and an injection port temperature of 140 °C.

Based on this platform, pyrolysis experiments of the $C_6F_{12}O$-N_2 gas mixture are carried out at different temperatures to measure the pyrolysis rate and major product concentrations as functions of temperature, providing experimental data to support the quantum chemical calculations.

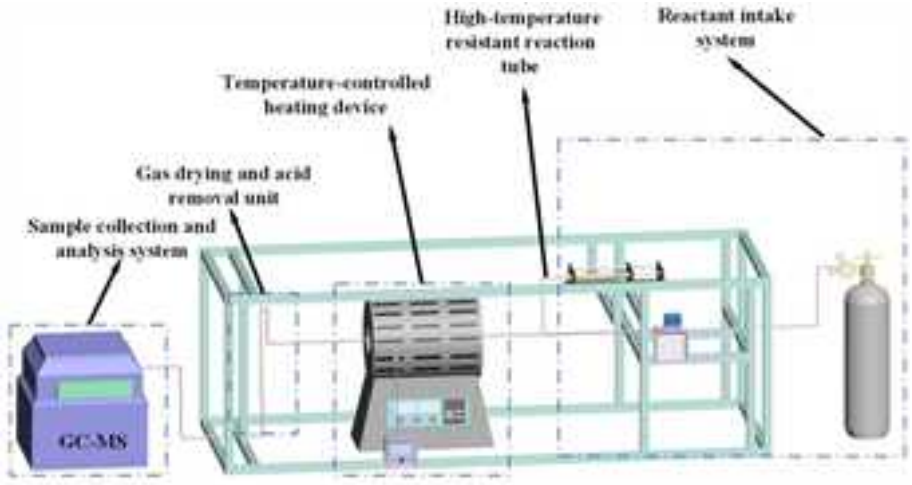

Fig. 1. 3D schematic diagram of thermal pyrolysis experimental platform.

2.2. Gaussian computational details

To investigate the intrinsic bond dissociation behavior of the $C_6F_{12}O$ molecule and identify the energetically preferred pyrolysis pathways, quantum chemical calculations are carried out using Gaussian 16 software. Obtaining bond dissociation energies through structural optimization calculations of isolated $C_6F_{12}O$ molecules in the gas phase at 0 K to determine the relative strengths of different bonds is a common method in DFT calculations. The hybrid functional B3LYP/6–311++G (d,p) basis set is employed throughout the study. This hybrid functional with a triple-ζ basis including diffuse and polarization functions has been widely used for SF_6-based insulating gases and perfluorinated ketones and has been shown to yield sufficiently accurate molecular structures and energies when compared with higher-level methods or experimental data [21,22]. Geometry optimization is performed under standard convergence criteria, and vibrational frequency analysis is conducted to ensure the obtained structure corresponds to a true local minimum on the potential energy surface. No imaginary frequencies are found in the optimized structure.

To evaluate potential bond scission reactions, homolytic breaking energies for all relevant C—C and C—F bonds are computed [21]. The dissociation energy (BDE) is calculated as the enthalpy difference between the parent molecule and its radical products, in their respective optimized geometries, to provide insights into their reactivity and stability. The quantum chemical results are subsequently used to map out primary pyrolysis channels and interpret the experimental and simulation findings. These theoretical pathways serve as a reference for identifying major reaction intermediates and for evaluating the thermal stability hierarchy of different molecular moieties within $C_6F_{12}O$ [23,24].

2.3. ReaxFF-MD simulation details

Quantum chemical methods can accurately study chemical reactions, but are computationally expensive and difficult to apply to the dynamics of large molecular systems. ReaxFF-MD is a simulation method that combines a reactive force field with molecular dynamics to investigate atomic interactions and chemical reaction kinetics in complex systems. The force field describes bond breaking and formation through relationships between bond order and bond length, with its potential energy function including terms for bond energy, over-coordination and under-coordination, valence angle, penalty energies, torsion, conjugation, and non-bonded interactions (van der Waals and Coulomb interactions), enabling high-precision simulation of chemical reactions [25–27]. The ReaxFF parameters used in this study are based on those developed by Li et al., which have been validated to be reliable for this system [20].

$$E_{system} = E_{bond} + E_{over} + E_{under} + E_{val} + E_{pen} + E_{tors} + E_{conj} + E_{vdWaals} + E_{Coulomb} \quad (1)$$

Where E_{bond} represents to the bond energy, E_{over} and E_{under} are the energy contributions of the over and under coordinated atoms, E_{val}, E_{pen}, E_{tors}, E_{conj}, $E_{vdWaals}$ and $E_{Coulomb}$ are the valence angle term, penalty energy, torsion energy, conjugation effects of energy, non-bonded van der Waals interaction and Coulomb interaction. This E_{system} covers all energy items related to the system and can simulate the reaction process with high accuracy [28].

To further investigate the pyrolysis influencing mechanisms of the $C_6F_{12}O$-N_2 gas mixture, cubic cells with an edge length of 500 Å are constructed (as shown in Fig. 2). ReaxFF-MD simulations are performed in the NVT ensemble (constant number of atoms, volume, and temperature) for 1000 ps with a time step of 0.1 fs. According to previous simulation results, this simulation time is sufficient to model the pyrolysis behavior of $C_6F_{12}O$ accurately. Based on this setup, multiple simulation systems are constructed by varying the initial numbers of $C_6F_{12}O$ and N_2 molecules to set different mixing ratios. Different pressure conditions are achieved by adjusting the total number of gas molecules in the cell according to the ideal gas law. Each system is simulated under different temperature conditions. Using higher temperatures to accelerate reactions is a common strategy in ReaxFF-MD simulations to trigger sufficient bond-breaking and recombination events within a finite simulation time. According to the Arrhenius equation, it does not alter the reaction's fundamental mechanism but allows the same reaction pathway to occur on a shorter timescale. Therefore, this study employs high-temperature simulations to shorten the simulation time and observe a more complete reaction process. The specific parameters

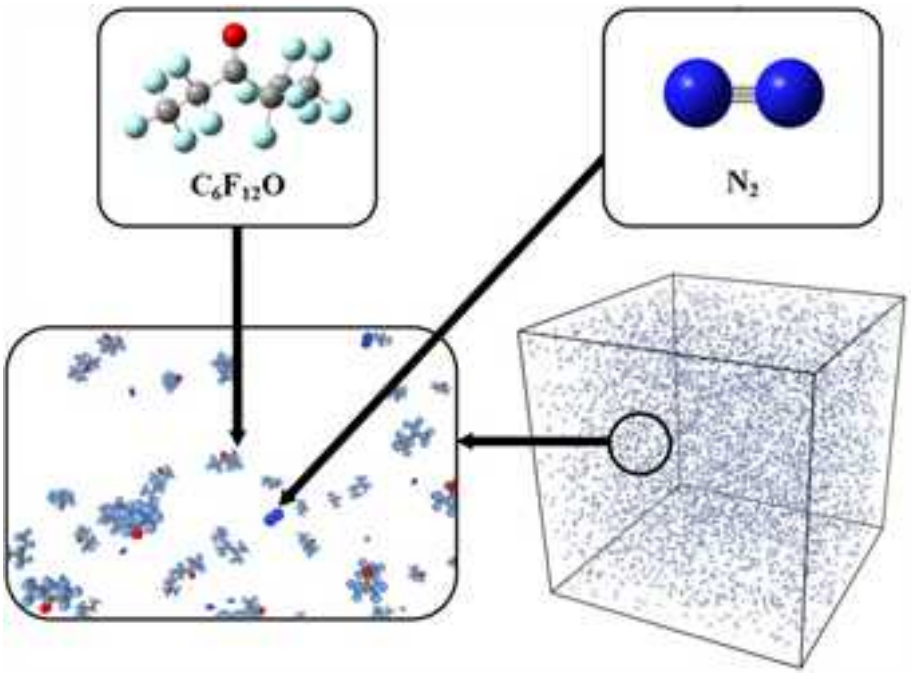

Fig. 2. Snapshot of the initial configuration of the $C_6F_{12}O$-N_2 system.

of each simulation system are listed in Table 1. In this study, experiments, DFT calculations, and ReaxFF-MD simulations are used as complementary tools at different scales. Although their temperatures and pressures differ, each method is applied in its most reliable regime, and their results are interpreted together to clarify the $C_6F_{12}O$-N_2 pyrolysis mechanism.

3. Results and discussion

3.1. Reaction pathway elucidation from quantum calculations

To provide a molecular-level basis for interpreting the pyrolysis behavior of $C_6F_{12}O$-N_2 mixtures, quantum chemical calculations were first carried out for isolated $C_6F_{12}O$ molecules. Gaussian 16 calculations using the B3LYP/6–311++G(d,p) method provided the optimized stable structure of $C_6F_{12}O$ (shown in Fig. 3).

From Table 2, the early-stage thermal pyrolysis of $C_6F_{12}O$ primarily involves cleavage of three carbon–carbon bonds: C3-C4, C2-C3, and C4-C5/C6. The required bond dissociation energies for these bonds are 220.33, 232.10, and 287.93 kJ/mol, respectively, and the corresponding products are $C_3F_7\cdot$ + $C_3F_5O\cdot$, $C_2F_5\cdot$ + $C_4F_7O\cdot$, and $CF_3\cdot$ + $C_5F_9O\cdot$, respectively. Based on these three reaction pathways and the distribution of the pyrolysis products, the main pyrolysis reaction pathways of the $C_6F_{12}O$-N_2 mixture were proposed as shown in Fig. 4.

Under high-temperature conditions, although terminal C—C bonds (e.g., C1-C2) can break to generate CF_3 radicals, their dissociation energy is significantly higher than that of C—C bonds adjacent to the carbonyl group. Therefore, pyrolysis is mainly initiated by the breaking of weaker bonds near the carbonyl group, with the breaking of the C1-C2 bond occurring as a secondary pathway in the initial stage, yielding CO and alkyl radicals such as $C_3F_7\cdot$, $C_2F_5\cdot$, and $CF_3\cdot$. These larger molecular radicals, due to their polarized internal bond energy distribution, further break down under thermal excitation to produce highly reactive small radicals such as $CF_3\cdot$, $CF_2\cdot$, and F· [29,30]. In hydrocarbon flames, the chain reaction is maintained by active free radicals such as H·, O·, and OH·. The key chemical fire suppression mechanism of $C_6F_{12}O$ and related fluorinated fire extinguishing agents is that the highly electronegative fluorinated free radicals generated during thermal pyrolysis readily react with the active free radicals in the chain reaction, forming stable products such as HF and COF_2. This reduces the total amount of free radicals, weakens the chain combustion reaction, and consequently reduces the flame propagation speed and heat release rate [12].

Moreover, at relatively lower temperatures, larger radicals such as $C_2F_5\cdot$ and $C_3F_7\cdot$ may undergo coupling reactions to form high molecular weight neutral products, such as C_6F_{14}, C_5F_{12}, C_4F_{10}, and C_3F_8. These products function as important intermediates in the mid-stage of pyrolysis, forming prominently in the medium-temperature range (approximately 500–700 °C). As the temperature increases further, they crack, releasing more small radicals and continuing to interrupt the combustion chain reaction.

Table 1
Parameters of the simulation system.

Number of molecules	Box size (Å)	Pressure (mPa)	Temperature (K)	timestep (fs)	Total simulation time(ps)
1000 $C_6F_{12}O$ / 2333 N_2			800 1200 1600 2000 2400 2800		
1667 $C_6F_{12}O$ / 1666 N_2		0.1	2800		
2333 $C_6F_{12}O$ / 1000 N_2			2800		
3333 $C_6F_{12}O$ / 0 N_2	500 × 500 × 500		2800	0.1	1000
1500 $C_6F_{12}O$ / 3500 N_2		0.15	2400		
2000 $C_6F_{12}O$ / 4666 N_2		0.2	2400		
2500 $C_6F_{12}O$ / 5833 N_2		0.25	2400		
3000 $C_6F_{12}O$ / 6999 N_2		0.3	2400		

Fig. 3. Schematic diagram of $C_6F_{12}O$ molecular structure.

Table 2
Bonds dissociation energy and reactions of $C_6F_{12}O$.

Atom 1	Atom 2	BDE(kJ/mol)	Bond dissociation reaction
C1	F	438.79	$C_6F_{12}O \rightarrow C_6F_{11}O\cdot + F\cdot$
	C2	246.21	$C_6F_{12}O \rightarrow CF_3\cdot + C_5F_9O\cdot$
C2	F	367.52	$C_6F_{12}O \rightarrow C_6F_{11}O\cdot + F\cdot$
	C3	232.10	$C_6F_{12}O \rightarrow C_2F_5\cdot + C_4F_7O\cdot$
C3	O7	966.41	$C_6F_{12}O \rightarrow C_6F_{12}\cdot + O\cdot$
	C4	220.33	$C_6F_{12}O \rightarrow C_3F_7\cdot + C_3F_5O\cdot$
C4	F	355.84	$C_6F_{12}O \rightarrow C_6F_{11}O\cdot + F\cdot$
	C5/C6	287.93	$C_6F_{12}O \rightarrow CF_3\cdot + C_5F_9O\cdot$
C5/C6	F	434.29	$C_6F_{12}O \rightarrow C_6F_{11}O\cdot + F\cdot$

3.2. Experimental characterization of $C_6F_{12}O$-N_2 thermal pyrolysis

Based on the preferred bond-breaking pathways identified by DFT in Section 3.1, high-temperature pyrolysis experiments were carried out to examine the product distribution of these molecular processes under macroscopic conditions. $C_6F_{12}O$-N_2 mixtures with a fixed volume ratio of 1:9 were passed through the heated zone of the tubular furnace at 450–750 °C with an effective residence time of approximately 4 s. Fig. 5 shows the total ion chromatograms of the pyrolysis gas products under these conditions.

When the temperature was below 450 °C, $C_6F_{12}O$ (peak at t = 15.1 min) underwent almost no pyrolysis. When the temperature rose to 550 °C, trace amounts of products began to appear: C_5F_{12} (t = 14.5 min), C_4F_{10} (t = 14.1 min), and C_6F_{14} (t = 15.5 min). As the temperature increased further, the extent of $C_6F_{12}O$ pyrolysis intensified, and the concentration of C_6F_{14} gradually decreased. Below 650 °C, the main pyrolysis products were C_5F_{12}, C_4F_{10}, C_3F_8 (t = 13.8 min), and C_3F_6 (t = 14.2 min). When the temperature reached 700 °C, the volume fraction of C_5F_{12} dropped from 44% to 24%, and C_4F_{10} (t = 14.9 min) appeared, but this peak gradually disappeared with further heating. Upon continued heating, $C_6F_{12}O$ was almost completely pyrolyzed, and no new C_5F_{12} was generated. Because C_5F_{12} has poor thermal stability, it easily cracked into more low-molecular-weight products at high temperatures,

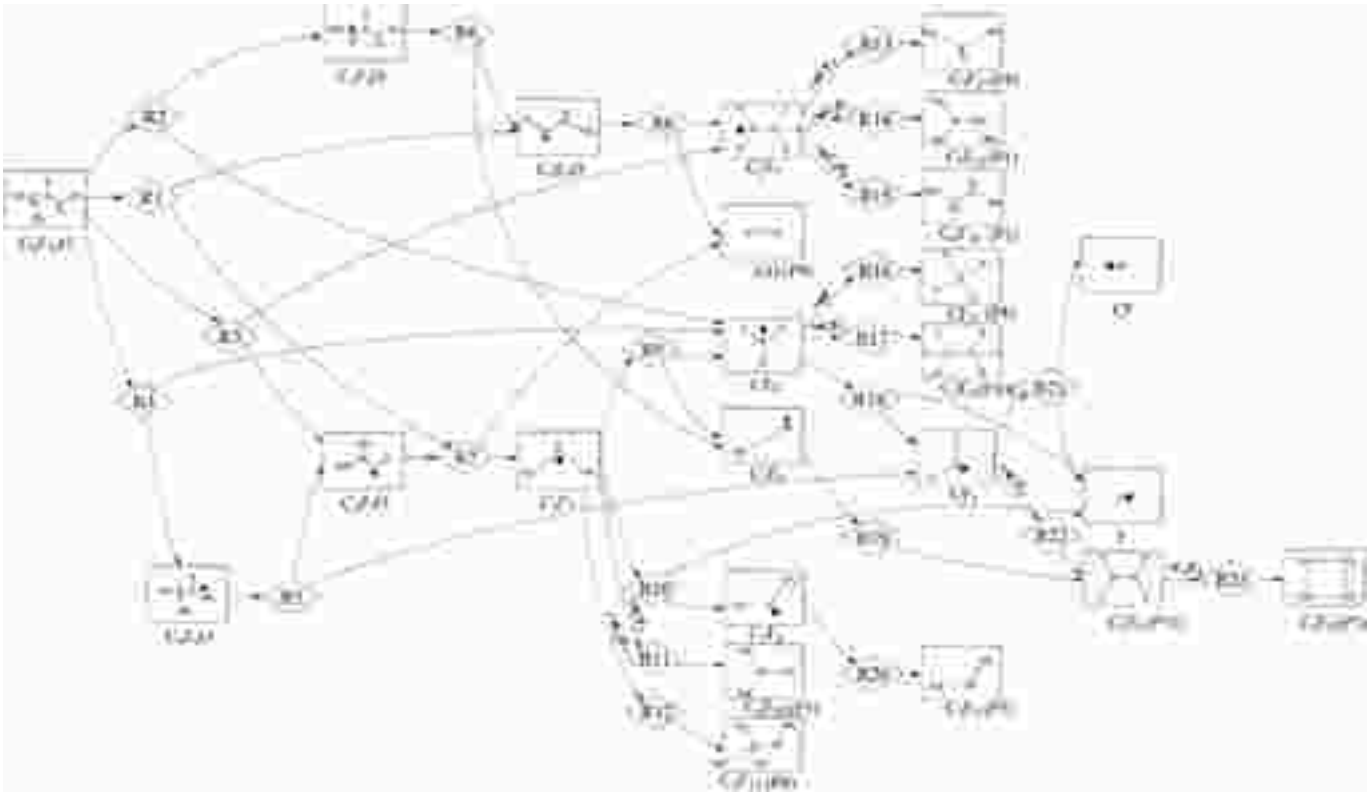

Fig. 4. Main pyrolysis reaction paths of $C_6F_{12}O$-N_2 mixed gas.

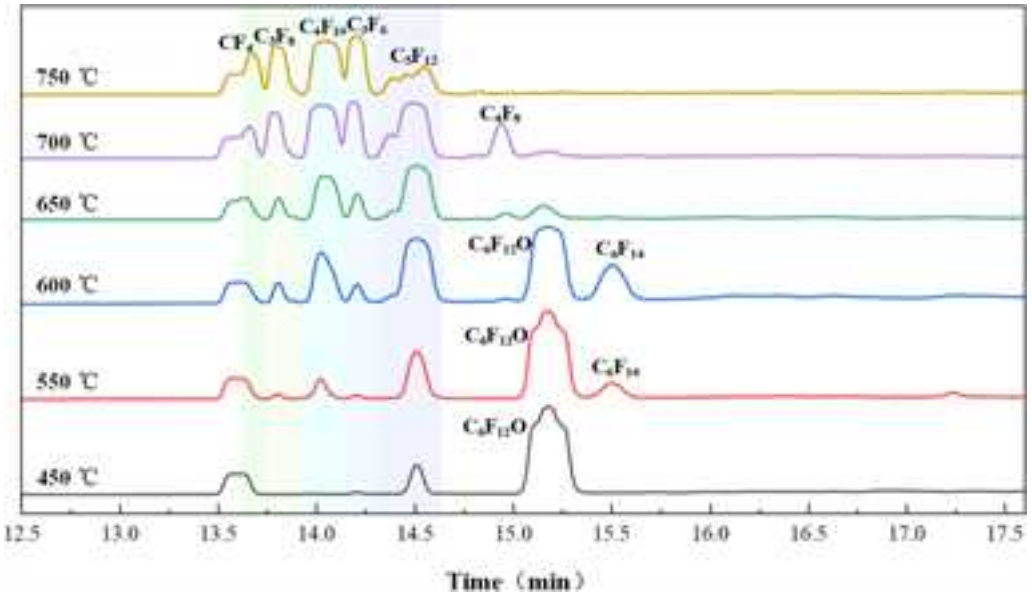

Fig. 5. Ion current chromatogram of pyrolysis gas products.

causing its volume fraction to decrease rapidly. When the temperature exceeded 750 °C, the variety of pyrolysis products further diminished, with mainly low-molecular-weight fluorocarbons such as CF_4 (t = 13.7 min), C_4F_{10}, C_3F_8, and C_3F_6 remaining [31]. At medium temperatures (550–650 °C), the dominant fluoroalkanes C_5F_{12} and C_6F_{14} originate primarily from the recombination of larger free radicals C_3F_7· and C_2F_5·. At higher temperatures, the increase in fluoroalkanes CF_4 and C_3F_6, and C_3F_8 reflects the further cracking of these high-fluoroalkanes to generate free radicals such as CF_3· and CF_2·, which in turn generate short-chain fluoroalkanes.

3.3. Parametric effects on pyrolysis

3.3.1. Effect of temperature on pyrolysis ratio and radical evolution

To better understand the impact of different operating parameters on the pyrolysis of mixed gases, it is necessary to conduct pyrolysis simulations of systems with a large number of molecules. Temperature is one of the most critical parameters influencing the pyrolysis behavior of

halogenated extinguishing agents. To investigate the effect of temperature on the pyrolysis behavior of the $C_6F_{12}O$–N_2 gas mixture, a series of ReaxFF–MD simulations were conducted. Fig. 6 shows the system's potential energy as a function of simulation time at different temperatures. It is evident that the system's potential energy steadily rises over time, suggesting that the overall pyrolysis process of the $C_6F_{12}O$-N_2 gas mixture is endothermic. From the simulation results, the pyrolysis ratio of $C_6F_{12}O$ at different temperatures over time was obtained, as shown in Fig. 7. The results show that below 1200 K, $C_6F_{12}O$ hardly pyrolyzes at all. With increasing temperature, the pyrolysis rate increases significantly: about 50% of $C_6F_{12}O$ pyrolyzes at 1600 K, ~94% at 2000 K, ~99.4% at 2400 K, and ~ 100% at 2800 K, with complete pyrolysis reached in approximately 28.7 ps. This trend indicates that as temperature increases, the pyrolysis rate of $C_6F_{12}O$ rises rapidly and the reaction intensifies. Therefore, temperature is a key factor affecting the chemical fire suppression performance of the $C_6F_{12}O$-N_2 gas mixture.

Fig. 8 shows the types and quantities of the major fragments produced from the $C_6F_{12}O$-N_2 gas mixture after pyrolysis at different temperatures. The simulation results indicate that the main fragments generated by pyrolysis include F·, CF·, CF_2·, CF_3·, CF_4, CO, C_2F_5·, C_3F_7·, and C_5F_9O·. Among these, the generation of C_3F_7·, C_5F_9O·, and C_2F_5· corresponds to the R_1, R_2, and R_3 pathways shown in Fig. 5, respectively. At lower simulation temperatures, the formation trends of CF_3· and C_5F_9O· radicals remained stable over time, with pyrolysis mainly following the R_2 pathway, which involves breaking the C4-C5/C6 bonds. As temperature increases, the formation rate of C_3F_7· radicals rises significantly, and their levels continue to grow without declining. This suggests that at higher temperatures, the initial pyrolysis of the $C_6F_{12}O$-N_2 gas mixture is primarily governed by the R_1 pathway, involving breaking the C3-C4 bonds. At this stage, the formation rate of C_3F_7· surpasses its consumption rate. This observation aligns with the bond energy calculations.

As the pyrolysis reaction proceeds and temperature increases, the quantities of the fragments F·, CF·, CF_2·, CF_3·, CF_4, and CO increase markedly. This is because the increased system energy increases molecular kinetic energy, causing the originally stable, high-energy C—C and C—F bonds in the $C_6F_{12}O$ molecule to break. The resulting larger radicals such as C_2F_5·, C_3F_7·, and C_5F_9O·, undergo further pyrolysis reactions to form highly active small intermediates. As the pyrolysis reaction advances, these small intermediates can polymerize or recombine to form more stable chemical species (denoted as P1-P11) and accumulate large amounts of fluorinated products. These simulation results

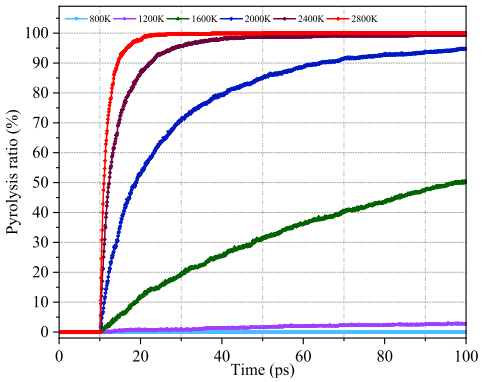

Fig. 7. Pyrolysis ratio of $C_6F_{12}O$ molecules at different temperatures.

are consistent with the product distribution observed in the experiments.

The ReaxFF-MD simulations complement the DFT and experimental results. The simulations confirm that the C—C bonds near the carbonyl group are activated first, generating C_3F_7· and C_2F_5· radicals as predicted by DFT, and these radicals subsequently fragment and recombine to produce fluorocarbons, which were detected in the formation experiment, indicating that this simulation method can replicate the pyrolysis process of the $C_6F_{12}O$-N_2 gas mixture. The simulations clearly show that as temperature increases, the initial pyrolysis rate of $C_6F_{12}O$ molecules accelerates significantly, triggering more intense chain reactions that produce many molecular fragments. At the same time, high temperature influences the pathways and rates of radical reactions, ultimately altering the distribution of major stable products as well as the concentration and lifetime of key intermediates.

Combining DFT calculation results, pyrolysis experimental results, and simulated fragment distribution results, it is shown that the flame-retardant effect of $C_6F_{12}O$ originates from the combined effect of physical cooling and chemical inhibition. When a $C_6F_{12}O$-N_2 agent is released into a fire zone, it first absorbs heat through vaporization of liquid droplets, and then absorbs additional heat during pyrolysis via endothermic cleavage and recombination of C—C and C—F bonds, thereby lowering the local gas temperature. The DFT and ReaxFF-MD results show that the dominant initial scission steps involve bonds adjacent to the carbonyl group and lead to fluorinated fragments such as CF_3·, C_2F_5·, and C3F7·, consistent with these endothermic pyrolysis

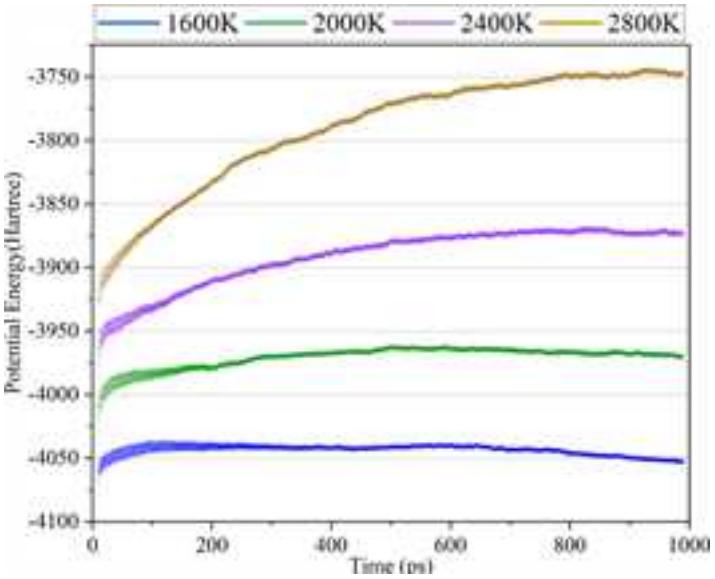

Fig. 6. The change of potential energy with time under different temperature conditions.

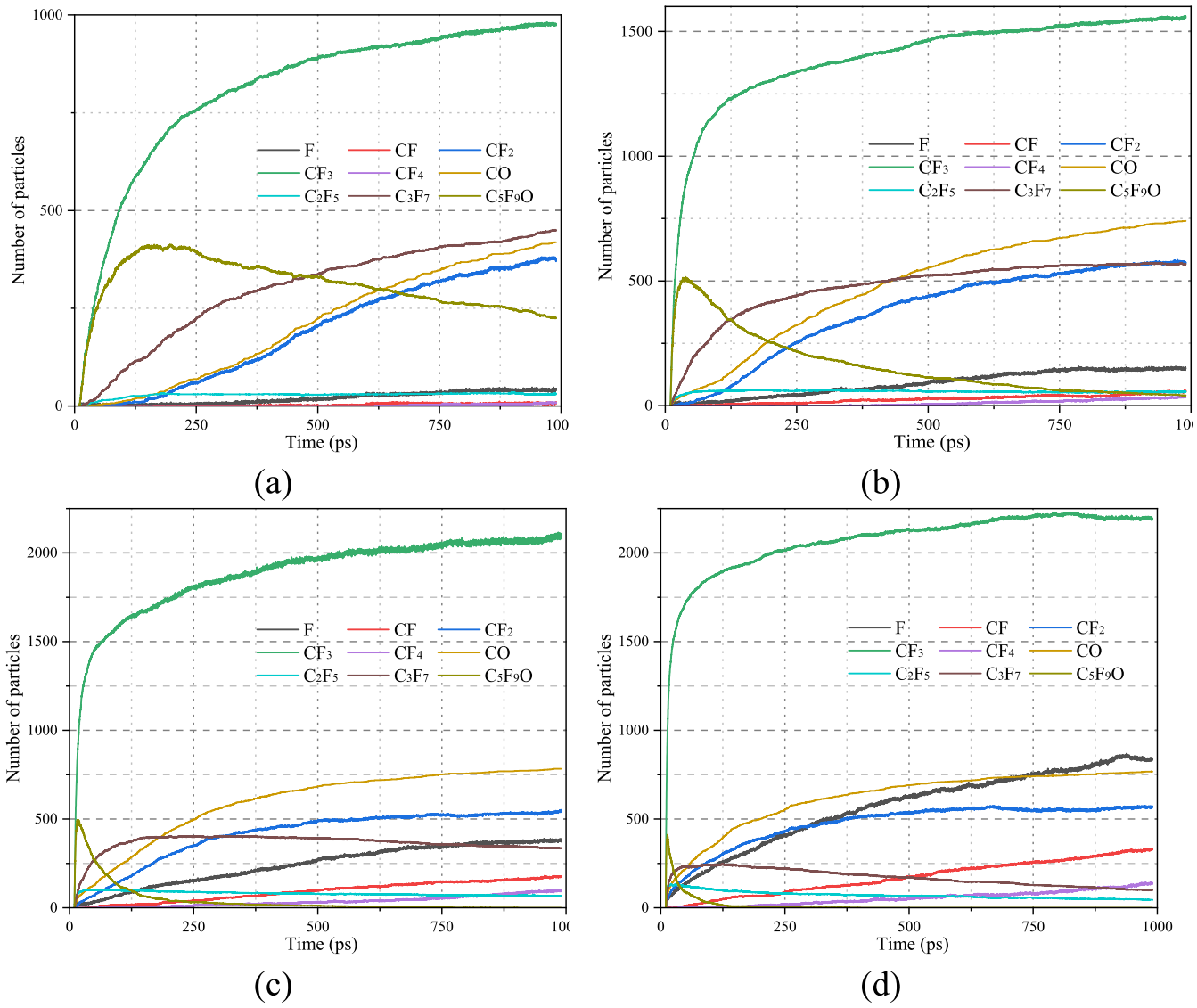

Fig. 8. Number of major pyrolysis particles of $C_6F_{12}O$-N_2 gas mixtures at different temperatures [(a)1600 K, (b) 2000 K, (c) 2400 K, (d) 2800 K].

pathways. The pyrolysis of the $C_6F_{12}O$-N_2 mixture thus exhibits a typical radical-dominated chain-reaction behavior, small radicals such as CF_3·, F· and related species generated in the early stage efficiently capture active combustion radicals (H·, O·, OH·), blocking chain-branching reactions. In the intermediate stage, larger radicals couple to form saturated products that can subsequently crack to release additional small radicals, while in the later stage, further product pyrolysis remains endothermic and slows the combustion rate. In parallel, the formation of species such as CO, COF_2 and C_3F_6, together with the inert dilution effect of N_2, effectively reduces the concentration and activity of oxygen and chain carriers in the flame zone. These processes act cooperatively to cool the flame, deplete key radicals and dilute reactants, providing mechanistic support for the multiple fire-suppression effects of $C_6F_{12}O$-N_2 mixtures.

3.3.2. *Effect of mixing ratio on pyrolysis ratio and radical evolution*

To understand the role of N_2 and its interaction with $C_6F_{12}O$, a series of simulations were carried out with different mixing ratios at a fixed high temperature (2800 K). The mixing ratio directly influences the molecular density of active species and the frequency of intermolecular collisions, thereby affecting both the initiation and propagation stages of pyrolysis.

As shown in Fig. 9(a), at 2800 K, increasing the proportion of N_2 in the gas mixture initially promotes the pyrolysis rate of $C_6F_{12}O$. For instance, In a mixture with a $C_6F_{12}O$:N_2 ratio of 3:7, the pyrolysis ratio at 15 ps reaches approximately 91.9%, whereas in the 5:5 and 7:3 mixtures, the pyrolysis ratios are 83.0% and 71.7%, respectively. The underlying reason for this observation can be attributed to the thermal conductivity and energy redistribution characteristics of N_2. As an inert gas with relatively low heat capacity at elevated temperatures, N_2 enhances energy transfer efficiency in the system, thereby facilitating the early-stage activation of $C_6F_{12}O$ molecules.

However, the effect of N_2 is nonlinear. Fig. 9(b) illustrates the temporal evolution of C_3F_7· radicals at different mixing ratios. In the later stages of pyrolysis, the dominance of inert N_2 molecules hinders the continuation of radical chain reactions by reducing the effective collision rate between reactive species. This suggests that while N_2 aids in thermal regulation and can reduce the required agent concentration, an optimal balance must be maintained to preserve the system's ability to generate and sustain active radicals.

From a mechanistic perspective, N_2 plays a dual role. First, it enhances thermal homogeneity and moderates the early energy distribution, facilitating bond activation in $C_6F_{12}O$. Second, due to its inert nature, it does not participate in radical quenching or recombination,

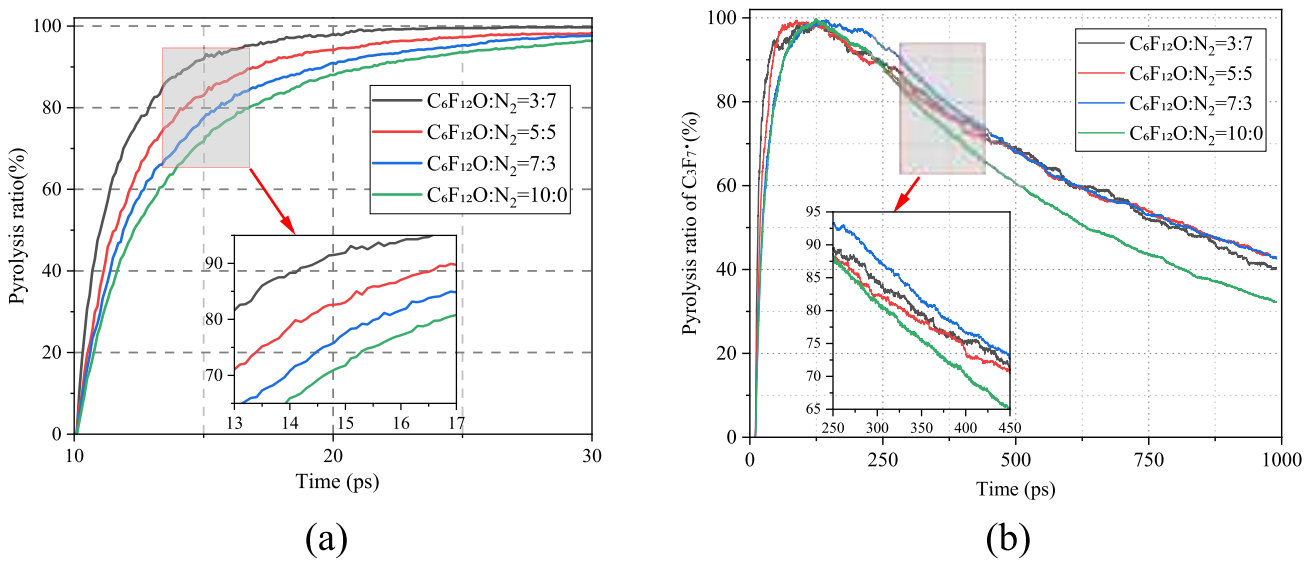

Fig. 9. Pyrolysis ratios of $C_6F_{12}O$ and C_3F_7· molecules at different mixing ratios at 2800 K (a) $C_6F_{12}O$ (b) C_3F_7·.

and excessive presence introduces a dilution effect, which can ultimately suppress the flame-inhibiting radical population. These findings underscore the importance of tailoring the mixing ratio for different fire scenarios, particularly in confined or high-pressure environments.

Additionally, since N_2 acts primarily through physical effects like dilution and cooling, its use in combination with $C_6F_{12}O$ may help mitigate the formation of toxic byproducts by lowering peak flame temperatures [32]. As a result, the $C_6F_{12}O$–N_2 system offers potential for optimized extinguishment performance with reduced environmental impact, provided that the mixture is formulated within an effective concentration window.

3.3.3. *Effect of pressure on pyrolysis ratio and radical evolution*

Pressure is another key variable that influences both the thermodynamic behavior and kinetic pathways of gas-phase pyrolysis. In this study, simulations were conducted at five nominal pressure conditions of 0.1 MPa, 0.15 MPa, 0.2 MPa, 0.25 MPa and 0.3 MPa as shown in Fig. 10(a). The results indicate that increasing the pressure significantly reduces the pyrolysis rate of $C_6F_{12}O$, at 20 ps, the pyrolysis ratio is about 86.7% at 0.1 MPa, about 80.6% at 0.2 MPa and only 71.6% at 0.3 MPa. Fig. 10(b) shows the evolution of the generation rate of C_2F_5· radicals over time at different pressures. As the gas density increases, the mean free path between molecules decreases, the diffusion of radicals is restricted, and the effective collision frequency between molecules increases, making radicals more likely to react. However, in a high-pressure environment, the energy distribution of the system tends to be uniform, which also inhibits the ability of $C_6F_{12}O$ molecules to acquire localized high energy to overcome high energy barriers. This is unfavorable for activating main breaking pathways such as the C3-C4 bond, suppressing the continuous generation of key radicals along the main pyrolysis channels, and thus reducing the overall pyrolysis efficiency.

Therefore, pressure exhibits a dual effect on the pyrolysis behavior of the $C_6F_{12}O$-N_2 gas mixture, moderately increasing pressure helps to ignite the chain reaction and increases the rate of radical production, but excessively high pressure may restrict the activation of high-energy reaction channels, suppress the main breaking pathways and radical cycles, and reduce the pyrolysis activity and fire suppression effectiveness of the gas mixture. In practical fire suppression applications, especially in enclosed environments such as aircraft cargo holds, high-pressure conditions may unintentionally inhibit the rapid activation of the extinguishing agent. This could potentially delay the formation of flame-inhibiting radicals during the critical early moments of fire development. In summary, pressure management is crucial for optimizing suppression performance. System designers should avoid excessive pressurization when configuring storage or discharge mechanisms and

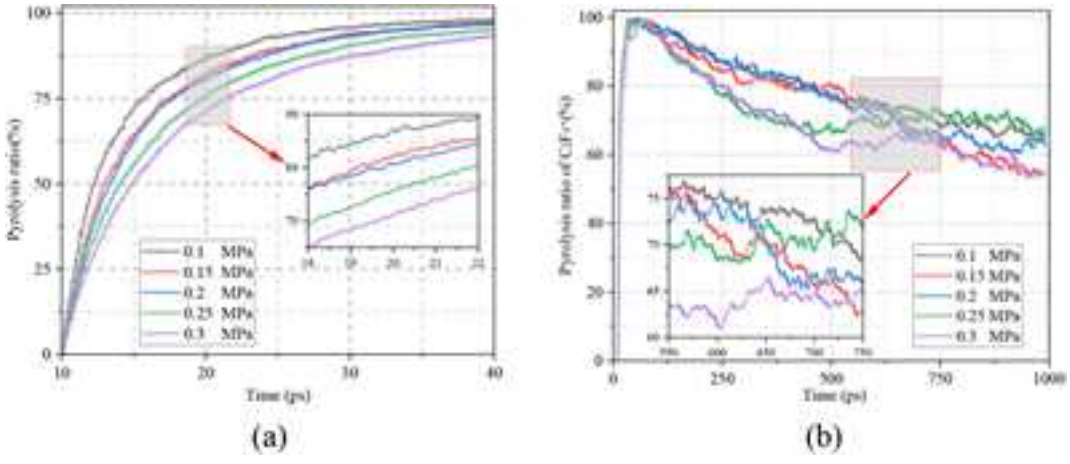

Fig. 10. Pyrolysis ratio of $C_6F_{12}O$ molecules at different pressures at 2400 K (a) $C_6F_{12}O$ (b) C_2F_5·.

instead aim for operational pressures that balance storage efficiency with chemical reactivity.

4. Conclusions

Through molecular dynamics simulations and experiments, the pyrolysis mechanism and influencing factors of the $C_6F_{12}O$-N_2 composite gas mixture have been studied. The main conclusions are as follows:

(1) DFT and GC–MS analyses clarify the main pyrolysis pathways and the radical chain mechanism in $C_6F_{12}O$–N_2 mixtures. Key intermediates (C_3F_7·, C_2F_5·, CF_3·) were identified as dual-role species in chain reactions, providing insight into microscopic reaction behavior.
(2) ReaxFF-MD simulations of temperature, $C_6F_{12}O$–N_2 ratio, and pressure effects show that pyrolysis extent and product distribution trends qualitatively match experiments. The time-resolved evolution of radical species in simulations further corroborates the proposed reaction pathways.
(3) Pyrolysis and radical evolution are highly dependent on temperature, $C_6F_{12}O$–N_2 ratio, and pressure. Moderate N_2 accelerates initial $C_6F_{12}O$ pyrolysis, whereas excess N_2 dilutes the mixture and slows chain propagation. Similarly, moderate pressure promotes radicals, but very high pressure suppresses high-energy pathways.
(4) $C_6F_{12}O$–N_2 fire suppression arises from combined physical and chemical mechanisms: endothermic $C_6F_{12}O$ pyrolysis absorbs flame heat, and the released radicals efficiently scavenge flame-propagating species. Inert N_2 and stable fluorinated byproducts dilute reactive species, synergistically inhibiting combustion.

CRediT authorship contribution statement

Kai Wang: Supervision. **Dezheng Wang:** Writing – original draft, Data curation. **Bin Zheng:** Visualization, Investigation. **Wei Wang:** Writing – review & editing. **Biao Zhou:** Methodology, Conceptualization.

Declaration of competing interest

The authors declare that they have no known competing financial interests or personal relationships that could have appeared to influence the work reported in this paper.

Acknowledgment

This study was supported by the National Key Research and Development Program of China (2023YFC3010202),the Ordos Key Research and Development Program (No. YF20240026), the Beijing Nova Program (No. 202504841008) and Fundamental Research Funds for the Central Universities (No. 2025ZKPYAQ03).

Data availability

Data will be made available on request.

References

[1] Y. Ren, F. Bernard, V. Daële, A. Mellouki, Atmospheric fate and impact of perfluorinated butanone and pentanone, Environ. Sci. Technol. 53 (2019) 8862–8871, https://doi.org/10.1021/acs.est.9b02974.
[2] B. D'Anna, S.R. Sellevåg, K. Wirtz, C.J. Nielsen, Photolysis study of perfluoro-2-methyl-3-pentanone under natural sunlight conditions, Environ. Sci. Technol. 39 (2005) 8708–8711, https://doi.org/10.1021/es048088u.
[3] M.L. Alonso, R.M. Alonso, J.I. Lombraña, J. Izcara, J. Izagirre, Exploring the decomposition products of 1, 3, 3, 3-tetrafluoropropene and perfluoro-(3-methylbutan-2-one) gas mixtures in medium-voltage electrical switchgear as alternatives to SF6, ACS Omega 6 (2021) 21534–21542, https://doi.org/10.1021/acsomega.1c02512.
[4] B. Yu, X. Jiang, C. Zhang, P. Xu, D. He, J. Yu, Y. Cai, Study on ignition delay and reaction mechanism of RP-3/air combustion adding C6F12O, ACS Omega 8 (2023) 24362–24370, https://doi.org/10.1021/acsomega.3c01888.
[5] H. Xing, S. Lu, H. Yang, H. Zhang, Review on research progress of C6F12O as a fire extinguishing agent, Fire 5 (2022) 50, https://doi.org/10.3390/fire5020050.
[6] J. Yu, F. Guo, B. Yu, X. Jiang, Inhibition/promotion effect of C6F12O addition on premixed laminar RP-3/air flames, ACS Omega 8 (2023) 3429–3440, https://doi.org/10.1021/acsomega.2c07354.
[7] J.L. Pagliaro, G.T. Linteris, P.B. Sunderland, P.T. Baker, Combustion inhibition and enhancement of premixed methane–air flames by halon replacements, Combust. Flame 162 (2015) 41–49, https://doi.org/10.1016/j.combustflame.2014.07.006.
[8] Y. Cao, C. Liu, X. Xu, E. Huo, Y. Pu, Influence of water on HFO-1234yf oxidation pyrolysis via ReaxFF molecular dynamics simulation, Mol. Phys. 117 (2019) 1768–1780, https://doi.org/10.1080/00268976.2019.1592255.
[9] W. Liu, F. Zhao, M. Kong, S. Yin, H. Wang, X. Liu, Reaction mechanism of Lithium-ion battery fire extinguishing agent-Perfluorinated Hexanone oxidizes metal-Al, Fire Technol. 58 (2022) 2811–2823, https://doi.org/10.1007/s10694-022-01280-9.
[10] S. Tian, X. Jin, X. Zhang, X. Li, Z. Yuan, L. Chen, Study on thermal decomposition characteristics of C6F12O/O2/CO2 gas mixtures, AIP Advances. 12 (2022), https://doi.org/10.1063/5.0123968.
[11] Y. Li, X. Zhang, Y. Wang, Y. Li, Y. Zhang, Z. Wei, S. Xiao, Experimental study on the effect of O2 on the discharge decomposition products of C5-PFK/N2 mixtures, J. Mater. Sci. Mater. Electron. 30 (2019) 19353–19361, https://doi.org/10.1007/s10854-019-02297-7.
[12] X. Mu, H. Cong, Z. Yuan, Y. Bi, M. Bi, Study on the inhibitory effect and mechanism of perfluoro (2-methyl-3-pentanone) on the combustion of gasoline blended with biomass additives, Fuel 349 (2023) 128768, https://doi.org/10.1016/j.fuel.2023.128768.
[13] Y. Zhang, X. Zhang, Y. Li, Y. Li, Q. Chen, G. Zhang, S. Xiao, J. Tang, Effect of oxygen on power frequency breakdown voltage and decomposition characteristics of the C 5 F 10 O/N 2/O 2 gas mixture, RSC Adv. 9 (2019) 18963–18970, https://doi.org/10.1039/C9RA03275D.
[14] Y. Han, Y. Zhou, Y. Xiong, H. Yuan, B. Zhou, Study on the cooling efficiency of typical gas fire extinguishing agents, Fire Science and Technology. 44 (2025) 402.
[15] F. Ye, Y. Chu, P. Brault, D. Hong, S. Tian, Y. Li, S. Xiao, X. Zhang, Mechanism of O_2 influence on the decomposition process of the eco-friendly gas insulating medium C_4F_7N/CO_2, IEEE Trans. Dielectr. Electr. Insul. 31 (2024) 2407–2415, https://doi.org/10.1109/TDEI.2024.3355352.
[16] M. Diakostefanis, S. Sampath, A. Dinesh, R. Beuermann, A. Malkogianni, Nitrogen as an environmentally friendly suppression agent for aircraft cargo fire safety, J. Fire Sci. 39 (2021) 400–424, https://doi.org/10.1177/07349041211034456.
[17] C. Li, H. Bian, D. Ding, F. Huang, Z. Zhu, Enhancing safety in small confined spaces with thermally triggered fire-extinguishing microcapsules from microfluidics, Lab Chip 24 (2024) 904–912, https://doi.org/10.1039/D3LC00911D.
[18] M. Zhao, D. Han, X. Han, X. Yan, W. Rong, G. Zhang, Decomposition by-products of C6F12O/N2 and C6F12O/air mixed gases under AC 50Hz corona discharge, Adv. Technol. Electr. Eng. Energy. 37 (2018) 4–11, https://doi.org/10.12067/ATEEE1802026.
[19] Y. Li, X. Zhang, S. Xiao, Q. Chen, D. Wang, Decomposition characteristics of C5F10O/air mixture as substitutes for SF6 to reduce global warming, J. Fluor. Chem. 208 (2018) 65–72, https://doi.org/10.1016/j.jfluchem.2018.01.015.
[20] Y. Li, X. Zhang, S. Tian, S. Xiao, Y. Li, D. Chen, Insight into the decomposition mechanism of C6F12O-CO2 gas mixture, Chem. Eng. J. 360 (2019) 929–940, https://doi.org/10.1016/j.cej.2018.10.167.
[21] Y. Fu, X. Wang, X. Li, A. Yang, G. Han, Y. Lu, Y. Wu, M. Rong, Theoretical study of the decomposition pathways and products of C5-perfluorinated ketone (C5 PFK), AIP Adv. 6 (2016), https://doi.org/10.1063/1.4960988.
[22] H. Duzkaya, S. Dincer, M. Dincer, S. Tezcan, Theoretical investigation of neutral decomposition by-products of SF6+ CO2 mixture in the existence of H2O, Electr. Eng. 102 (2020) 1451–1467, https://doi.org/10.1007/s00202-020-00965-0.
[23] F. Wang, J. Liu, L. Zhong, B. Hai, Y. Zhou, N. Tang, L. Li, Theoretical analysis of the decomposition pathways and species of environmentally friendly insulation gas C6F12O based on the DFT and TST, Plasma Chem. Plasma Process. 41 (2021) 133–153, https://doi.org/10.1007/s11090-020-10129-4.
[24] T. Wang, P. Zhang, R. Pan, Investigation of the high temperature pyrolysis behavior of Perfluorohexanone as an environmental-friendly fire extinguishing agent, pin and Pan, Renming, Investigation of the High Temperature Pyrolysis Behavior of Perfluorohexanone as an Environmental-Friendly Fire Extinguishing Agent. (2024), https://doi.org/10.1002/(SICI)1099-1018(199803/04)22:2%3C47::AID-FAM630%3E3.0.CO;2-2.
[25] Y. Chen, H. Chen, J. Wang, Y. Huang, Chemical kinetics of hexamethyldisiloxane pyrolysis: a ReaxFF molecular dynamics simulation study, Int. J. Chem. Kinet. 54 (2022) 413–423, https://doi.org/10.1002/kin.21570.
[26] L. Xin, C. Liu, Y. Liu, E. Huo, Q. Li, X. Wang, Q. Cheng, Thermal decomposition mechanism of some hydrocarbons by ReaxFF-based molecular dynamics and density functional theory study, Fuel 275 (2020) 117885, https://doi.org/10.1016/j.fuel.2020.117885.
[27] Y. Wang, L. Zhou, Q. Mao, Z. Wang, H. Wei, Pyrolysis and oxidation of benzene and cyclopentadiene by NO x: a ReaxFF molecular dynamics study, Phys. Chem. Chem. Phys. 25 (2023) 13690–13701, https://doi.org/10.1039/D2CP04413G.
[28] A.C. Van Duin, S. Dasgupta, F. Lorant, W.A. Goddard, ReaxFF: a reactive force field for hydrocarbons, J. Phys. Chem. A 105 (2001) 9396–9409, https://doi.org/10.1021/jp004368u.

[29] X. Zhang, Y. Li, D. Chen, S. Xiao, S. Tian, J. Tang, R. Zhuo, Reactive molecular dynamics study of the decomposition mechanism of the environmentally friendly insulating medium C 3 F 7 CN, RSC Adv. 7 (2017) 50663–50671, https://doi.org/10.1039/C7RA09959B.
[30] X. Zhang, Y. Li, S. Xiao, J. Tang, S. Tian, Z. Deng, Decomposition mechanism of C5F10O: an environmentally friendly insulation medium, Environ. Sci. Technol. 51 (2017) 10127–10136, https://doi.org/10.1021/acs.est.7b02419.
[31] P. Han, Y. Xia, J. Tang, Z. Wei, S. Xie, C. Zhang, S. Xiao, Effect of O2 on partial discharge and decomposition characteristics of C5F10O/CO2/O2 gas mixture, AIP Adv. 12 (2022), https://doi.org/10.1063/5.0076346.
[32] K. Wang, D. Wang, B. Zhou, X. Wang, T. Chen, Study on the synergistic extinguishing effect of perfluorohexanone-nitrogen, Case Stud. Therm. Eng. 71 (2025), https://doi.org/10.3390/fire7120479.